



Since January 2020 Elsevier has created a COVID-19 resource centre with free information in English and Mandarin on the novel coronavirus COVID-19. The COVID-19 resource centre is hosted on Elsevier Connect, the company's public news and information website.

Elsevier hereby grants permission to make all its COVID-19-related research that is available on the COVID-19 resource centre - including this research content - immediately available in PubMed Central and other publicly funded repositories, such as the WHO COVID database with rights for unrestricted research re-use and analyses in any form or by any means with acknowledgement of the original source. These permissions are granted for free by Elsevier for as long as the COVID-19 resource centre remains active.

An Alumina Ceramic Total Talar Prosthesis for Avascular Necrosis of the Talus



Akira Taniguchi, MD, PhD*, Yasuhito Tanaka, MD, PhD

KEYWORDS

• Aseptic necrosis • Talus • Total talar prosthesis • Alumina ceramic

KEY POINTS

- The talus is surrounded by the tibia, fibula, calcaneus, and navicular, composing some joints in between with these bones.
- Customized alumina ceramic total talar prosthesis is an ideal implant for the replacement due to talar osteonecrosis.
- Preservation of joint function and prevention of leg length discrepancy are important to treat talar osteonecrosis.
- In the authors' experience of 55 ankles in 41 patients with talar osteonecrosis, both subjective and objective scale scores improved after the replacement with customized alumina ceramic total talar prosthesis.

INTRODUCTION

The talus is surrounded by the tibia, fibula, calcaneus, and navicular, and approximately 70% of its surface is covered with articular cartilage. The medial segment of the talus is supplied by the tarsal tunnel artery, branched by the posterior tibial artery. The head and neck of the talus are mainly supplied by the tarsal tunnel and anterior tibial arteries.^{1,2} However, avascular necrosis tends to occur in the talus because of poor blood supply from the periosteum.

The causes of talar osteonecrosis are trauma,^{3,4} excessive steroid use,⁵ alcohol,⁶ systemic lupus erythematosus,⁶ pancreatitis,⁷ hemophilia,^{8,9} and severe acute respiratory syndrome.¹⁰ The frequency of talar osteonecrosis associated with talar fracture has been reported to be approximately 10%, 40%, and 90% in Hawkins types 1, 2, and 3,¹¹ respectively. More recently, talar osteonecrosis frequency decreased to 64%, even in type 3, because of the improved surgical

Disclosure Statement: The authors have nothing to disclose.

Department of Orthopaedic Surgery, Nara Medical University, 840 Shijyo-cho, Kashihara, Nara 631-8522, Japan

* Corresponding author.

E-mail address: a-tani@naramed-u.ac.jp

Foot Ankle Clin N Am 24 (2019) 163–171

<https://doi.org/10.1016/j.fcl.2018.10.004>

1083-7515/19/© 2018 Elsevier Inc. All rights reserved.

foot.theclinics.com

techniques and implants.³ However, the frequency of talar osteonecrosis in patients with talar fracture dislocation is still higher. Steroid use increases the blood level of fat, which induces microcontusions, leading to osteonecrosis.⁵ Delanois and colleagues¹² reported that 20 of 24 subjects with traumatic talar osteonecrosis had a history of steroid therapy. However, no evidence supports the correlation.

Blair fusion used to be adapted for this condition because it uses the healthy talar neck.^{13,14} Although minimal discrepancy of the lower leg remains after this procedure, hindfoot instability and non union in the fixation site sometimes occurred. In some cases, iliac crest harvest and external fixator may be necessary.

The customized alumina ceramic talar prosthesis was developed in 1994 to compensate for the disadvantages of fusion treatments.^{15,16} The first-generation implant was a talar body prosthesis with a bone peg for cement fixation to the talar neck. However, some cases had loosening at the fixation site. In 2004, the second-generation implant was designed as a talar body prosthesis without a bone peg and was expected to perform the bearing function on the talar body. However, talar head rupture occurred in some cases because of higher pressure to the talar head. Therefore, total talar prosthesis was developed in 2005 and has been used since. In this article, diagnosis and treatment of talar osteonecrosis, as well as surgical technique for artificial talus implantation, are discussed.



Fig. 1. Radiograph of a 57-year-old man with a vascular necrosis of the talus. Otosclerosis is seen in the body of the talus.

DIAGNOSIS

An etiologic factor of osteonecrosis is that bone ischemia is induced by blood flow disturbance. The cycle of ossification, revascularization, and reabsorption is repeated for the healing system. In early-phase radiography, little difference is seen compared with healthy bone. Next, reabsorption revolves around the necrotic bone, which induces bone atrophy followed by decreased bone stock. In the center of osteonecrosis, sclerotic change appears because of blood flow disruption.

Radiographic staging of osteonecrosis was developed by Ficat and Arlet¹⁷ and was modified for the ankle by Mont and Colleagues¹⁸. Stage 1 is defined as no radiographic findings, stage 2 is defined as cystic lesion and/or sclerotic change in the talus, stage 3 is defined as crescent sign or collapse in the subchondral bone, and stage 4 is defined as joint space narrowing.

In some patients with trauma to the talus, the clear zone can be recognized in the subchondral bone after 6 to 8 weeks of trauma, even in cases with initial sclerotic change, by the restoration of blood flow and that it is free from osteonecrosis (Hawkins sign).

Patients with atraumatic talar osteonecrosis usually consult physicians because of relatively minor ankle pain. Sclerotic change in the talar body would be observed even in cases without severe collapse in the talus (Fig. 1). The sagittal and coronal planes of a computed tomography (CT) image reveal sclerotic change in the bony structure of the talus (Fig. 2)¹⁹. Moreover, a 3-dimensional image makes the evaluation of the



Fig. 2. CT of the same patient. Otosclerosis is seen in the whole body of the talus.

collapse of the talar body and selection of the surgical option possible. In patients treated with artificial talus, CT of the contralateral ankle should be obtained to make a customized implant.

MRI is useful for the detection of early lesions.¹⁹ In the T1-weighted image, the lesion is visualized in the low-density area, reflecting loss of fatty bone marrow. In the T2-weighted image, the lesion is visualized in the high-density and low-density areas, reflecting bone marrow edema in the early and advanced stages, respectively. In the fat-suppressed T2-weighted image, a mixture of high-intensity and low-intensity areas is seen, reflecting bone marrow edema and necrosis, respectively (Fig. 3).

Bone scintigraphy has potential diagnostic power to detect the early phase.²⁰ Although other modalities evaluate only the local tissue, bone scintigraphy targets the whole body, which is an advantage for the diagnosis of atraumatic necrosis. The lesion has a cold area, reflecting the lack of uptake due to necrosis, and a hot area around the cold area reflecting the higher uptake results from reabsorption (cold in hot) (Fig. 4).

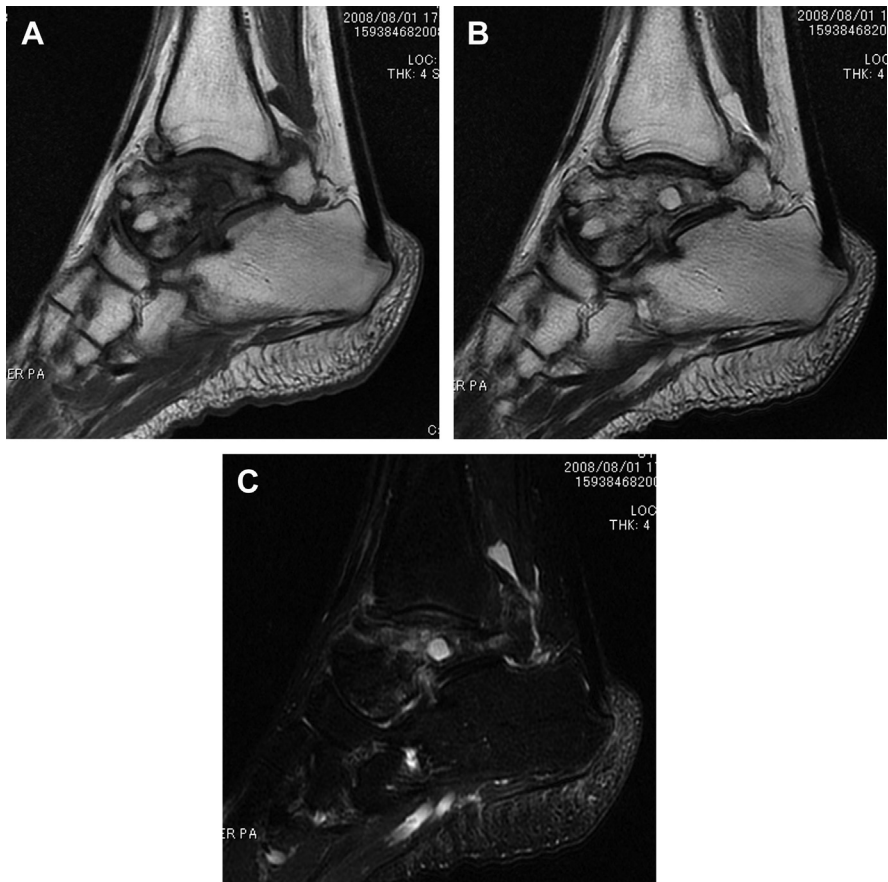


Fig. 3. MRI of a 52-year-old woman. (A) In the T1-weighted image, a low-density area is seen in the body of the talus. (B) In the T2-weighted image, a high-density area is seen in the body of the talus, and bony cyst is identified in it. (C) In fat-suppressed T2-weighted image, a mixture of high-intensity and low-intensity areas is seen, reflecting bone marrow edema and necrosis, respectively.

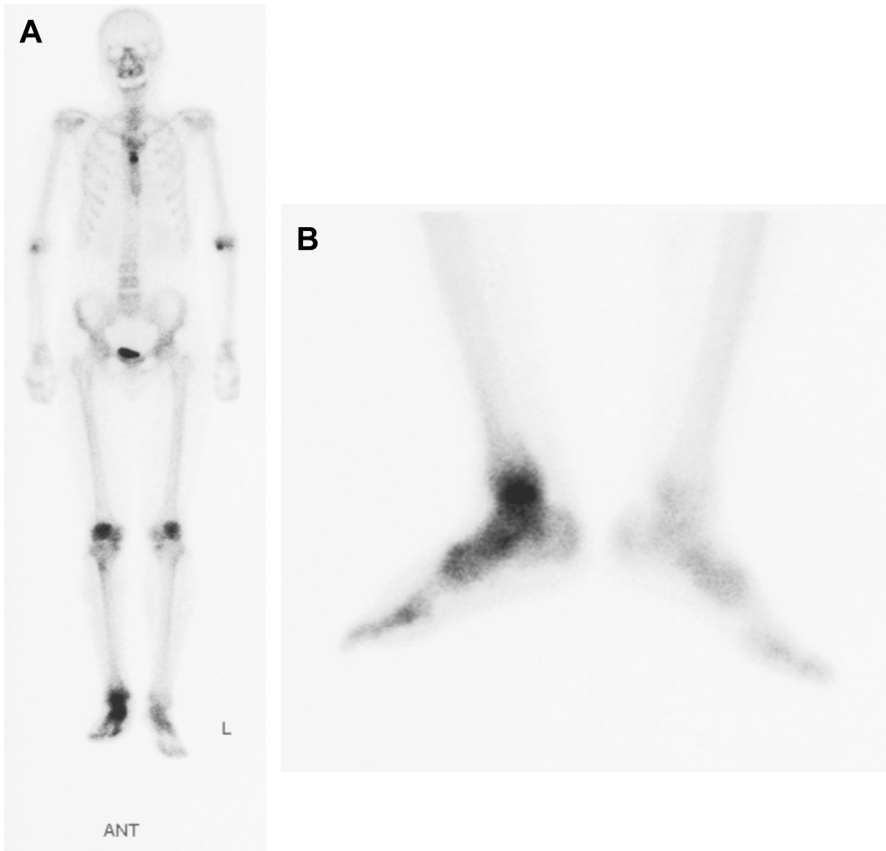


Fig. 4. ^{99m}Tc -HMDP bone scintigraphy of a 50-year-old man. (A) ^{99m}Tc -HMDP (hydroxymethylene diphosphonate) concentrates to the right talus. (B) The lesion has a cold area, reflecting the lack of uptake due to necrosis, and a hot area around the cold area, reflecting the higher uptake results from reabsorption (cold in hot).

TREATMENT

For patients with stage 1 or 2 without evidence of collapse, dislocation, or degenerative changes in the talus, nonweightbearing using crutches or a knee-bearing orthosis is indicated. Partial weightbearing is allowed after bone resorption is recognized because this indicates the restoration of the blood supply, whereas nonweightbearing may continue long-term in cases without findings of bone resorption.²¹ Surgical treatment is considered in patients not responding to conservative therapy.¹⁸ For patients with stage 1 or 2, core decompression technique would be used. Drills of 1.5 mm to 2.0 mm in diameter are inserted into the lesion 5 to 10 times from the posterolateral, lateral, or medial sides, or a drill of 4.0 mm in diameter is inserted 2 to 4 times to reduce the pressure in the lesion. Horst and colleagues²¹ reported decreased pain and improved ankle motion in 70% of subjects after this procedure.

For patients with stage 3 and 4, surgical treatment is usually selected, particularly in patients with talar collapse. Tibiocalcaneal fusion connecting the tibia and calcaneus

after resecting the collapsed talar body usually results in length discrepancy of the lower legs. Blair fusion connecting the tibia and talar neck with the fibula results in less discrepancy; however, long-term mounting of the external fixator is required to address instability in the fixation site.^{13,14} Recently introduced artificial talar prostheses prevent leg length discrepancy, preserve the joint function, and allow early weightbearing.^{15,16}

CT of the healthy side of the talus is obtained to make a customized implant. CT images are reconstructed in the pitch of 2 mm in the coronal and sagittal planes. The talar area is identified in each slice, the reconstructed image of the talus is reversed, and the implant is made using this image (Fig. 5A–F). The customized ceramic implant is produced in 4 to 5 weeks (Fig. 5G); therefore, preventing further collapse of the talus caused by weightbearing is necessary.

Under spinal or general anesthesia, a 10-cm skin incision is made in the anterior ankle. The extensor retinaculum is incised, avoiding damage to the superficial peroneal nerve, and the ankle is exposed between the flexor hallucis longus and tibialis anterior tendons. In addition, the talonavicular joint is exposed in the distal side. After the dissection of the joint capsule and ligaments, the talar neck is cut and the talar head is removed. The talar body is cut 1-cm thick on the coronal plane, dissecting the interosseous talocalcaneal ligament. Removal of the entire bone fragment without retaining small fragments in the surgical site is important. After irrigation of

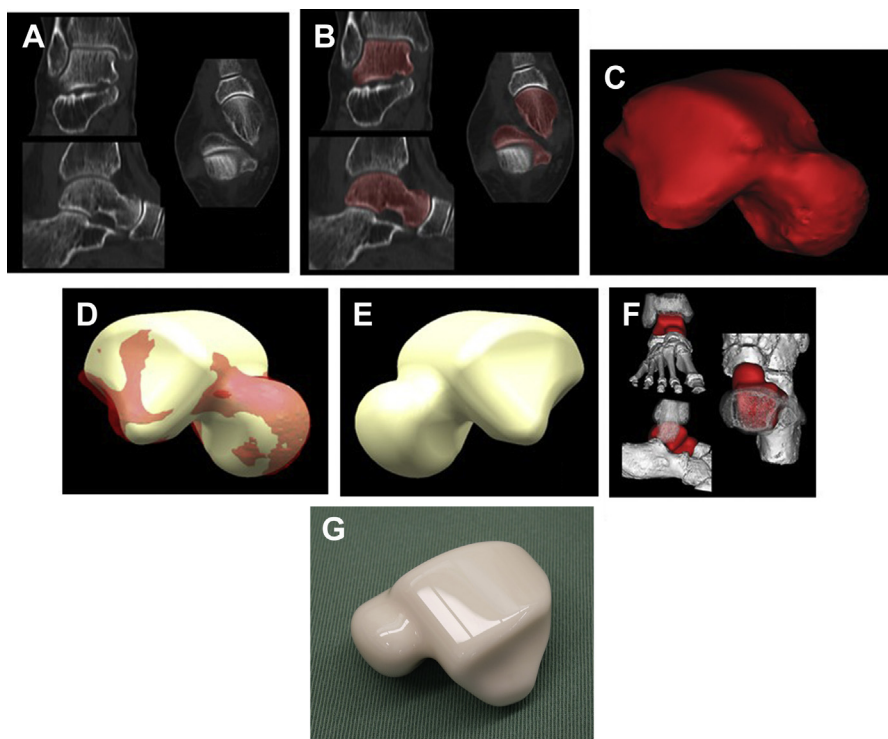


Fig. 5. Creating the customized artificial talus. (A) CT scan of the healthy side. (B) Distinction of the talus. (C) Rending and CAD (Computer Aided Designing) imaging. (D) Correction of CAD image. (E) Turnover of the image. (F) Simulation in the 3-dimensional CT. (G) Finished alumina ceramic total talar prosthesis.

the surgical site, the artificial talus is inserted with assistance of foot traction. The ankle, subtalar, and talonavicular joints are ranged to confirm good prosthetic fit. The surgical wound is closed following joint capsule repair (Fig. 6). A below-knee walking cast is applied for 3 weeks. Weightbearing is avoided in the first week, partial weightbearing is allowed in the second week, and full weightbearing is allowed in the third week (Fig. 7).

In the authors' experience of 55 ankles in 41 patients with talar osteonecrosis, the Japanese Society for Surgery of the Foot Ankle-Hindfoot Scale score improved from 42.2 plus or minus 17.4 to 89.1 plus or minus 8.6. In the subcategory of pain, score improved from 15.0 plus or minus 9.4 to 34.0 plus or minus 5.6, function score improved from 21.2 plus or minus 9.7 to 45.1 plus or minus 4.0, and alignment score improved from 6.0 plus or minus 2.8 to 9.8 plus or minus 0.9. Based on the Ankle Osteoarthritis Scale, the score for pain at its worst improved from a mean of 6.1 plus or minus 3.3 to 2.0 plus or minus 1.7. At final follow-up, ankle inversion stress radiography showed a talar tilting angle of 5.0° plus or minus 3.6° and an anterior drawer distance of 1.4 plus or minus 0.5 mm. Dislocation and migration of the implant were not observed.²²

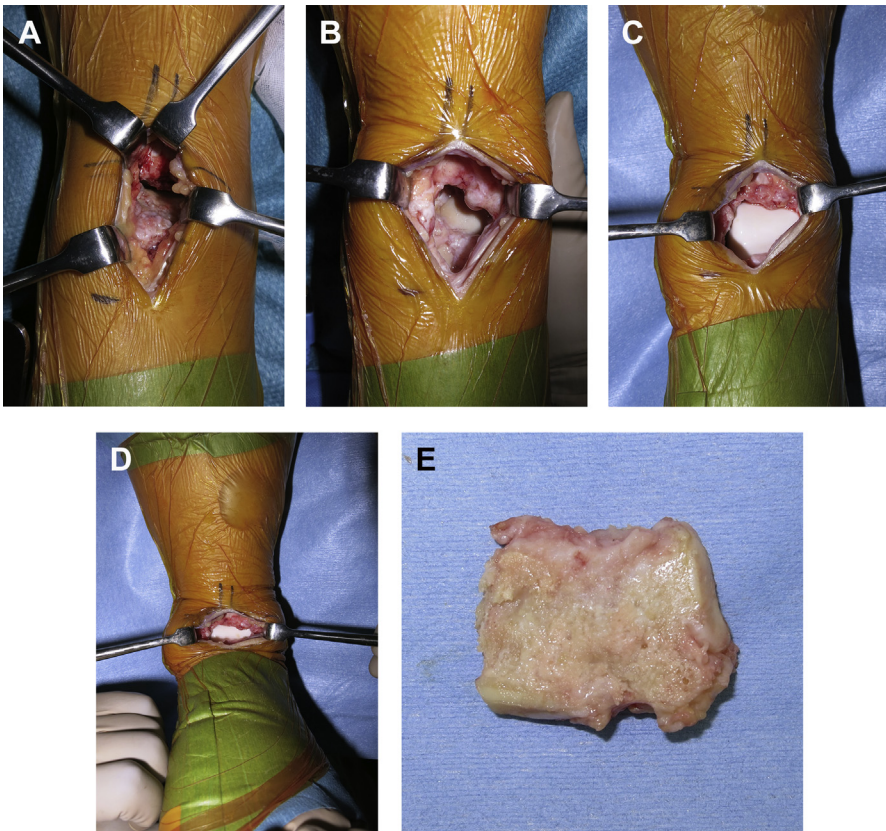


Fig. 6. Intraoperative findings of 64 year-old woman suffering from idiopathic talar necrosis. (A) The talar dome is collapsed and joint surface is widely degenerated. (B) The talus is completely removed. Artificial talar implant is inserted. (C) Plantar flexed position. (D) Dorsal flexed position. (E) Excised specimen. Talar dome is severely compressed and trabecula in the talar body has completely disappeared.



Fig. 7. Postoperative weightbearing radiography. (A) Anteroposterior view. (B) Lateral view.

In summary, the talus is surrounded by the tibia, fibula, calcaneus, and navicular, composing some joints in between with these bones. Customized alumina ceramic total talar prosthesis is an ideal implant for the treatment of severe talar osteonecrosis.

REFERENCES

1. Sanders RW, Lindvall E. Fractures and fracture-dislocation of the talus. In: Coughlin MJ, Mann RA, Saltzman CL, editors. *Surgery of the foot and ankle*. 8th edition. Philadelphia: Mosby Elsevier; 2007. p. 2074–136.
2. Gelberman RH, Mortensen WW. The arterial anatomy of the talus. *Foot Ankle* 1983;4:64–72.
3. Vallier HA, Nork SE, Barei DP, et al. Talar neck fractures: results and outcomes. *J Bone Joint Surg Am* 2004;86-A:1616–24.
4. Lindvall E, Haidukewych G, DiPasquale T, et al. Open reduction and stable fixation of isolated, displaced talar neck and body fractures. *J Bone Joint Surg Am* 2004;86-A:2229–37.
5. Adleberg JS, Smith GH. Corticosteroid-induced avascular necrosis of the talus. *J Foot Surg* 1991;30:66–9.
6. Harris RD, Silver RA. Atraumatic aseptic necrosis of the talus. *Radiology* 1973;106:81–3.
7. Baron M, Paltiel H, Lander P, et al. Aseptic necrosis of the talus and calcaneal insufficiency fractures in a patient with pancreatitis, subcutaneous fat necrosis, and arthritis. *Arthritis Rheum* 1984;27:1309–13.
8. Macnicol MF, Ludlam CA. Does avascular necrosis cause collapse of the dome of the talus in severe haemophilia? *Haemophilia* 1999;5:139–42.
9. Kemnitz S, Moens P, Peerlinck K, et al. Avascular necrosis of the talus in children with haemophilia. *J Pediatr Orthop B* 2002;11:73–8.

10. Hong N, Du XK. Avascular necrosis of bone in severe acute respiratory syndrome. *Clin Radiol* 2004;59:602–8.
11. DiGiovanni CW, Patel A, Calfee R, et al. Osteonecrosis in the foot. *J Am Acad Orthop Surg* 2007;15:208–17.
12. Delanois RE, Mont MA, Yoon TR, et al. Atraumatic osteonecrosis of the talus. *J Bone Joint Surg Am* 1998;80-A:529–36.
13. Blair H. Comminuted fractures and fracture dislocation of the body of the astragalus. *Am J Surg* 1943;59:37.
14. Lionberger DR, Bishop JO, Tullos HS. The modified Blair fusion. *Foot Ankle* 1982;3:60–2.
15. Tanaka Y, Takakura Y, Kadono K, et al. Alumina ceramic talar body prosthesis for idiopathic aseptic necrosis of the talus. *Bioceramic* 2002;15:805–8.
16. Kadono K, Tanaka Y, Sugimoto K, et al. Replacement of the body of the talus with alumina ceramic prosthesis for idiopathic aseptic necrosis. *Orthop Ceramic Implant* 2002;21:77–81 [in Japanese].
17. Ficat RP, Arlet J. Ischemia and necrosis of bone. Baltimore (MD): Williams and Wilkins; 1980. p. 171–82.
18. Mont MA, Schon LC, Hungerford MW, et al. Avascular necrosis of the talus treated by core decompression. *J Bone Joint Surg Am* 1996;78-B:827–30.
19. Pearce DH, Mongiardi CN, Fornasier VL, et al. Avascular necrosis of the talus: a pictorial essay. *Radiographics* 2005;25:399–410.
20. Shafa MH, Fernandez-Ulloa M, Rost RC, et al. Diagnosis of aseptic necrosis of the talus by bone scintigraphy. *Clin Nucl Med* 1983;8:50–3.
21. Horst F, Gilbert BJ, Nunley JA. Avascular necrosis of the talus: current treatment options. *Foot Ankle Clin N Am* 2004;9:757–73.
22. Taniguchi A, Takakura Y, Tanaka Y, et al. An alumina ceramic total talar prosthesis for osteonecrosis of the talus. *J Bone Joint Surg Am* 2015;97-A:1348–53.